

Interference and Elliptic Integrals

Niels Jansen

Scriptiebegeleiders:

Prof.dr.ir. Barry Koren
Prof.dr.ir. Tjerk Oosterkamp
Prof.dr. Bas Edixhoven

25 december 2011



Mathematisch Instituut, LION, Universiteit Leiden

Inhoudsopgave

1	Introduction	4
2	Closed Multiwalled Carbon Nanotubes	4
3	Models	5
3.1	2-D model	5
3.2	Linear model	7
3.3	Revisited model	8
3.4	Longitudinal Energy	9
4	Numerical Method	10
5	Results	11
6	Discussion	17
7	Conclusion	20
8	References	21
A	Pari/GP Codes	22
A.1	Code for calculating the phases with the 2-D model	22
A.2	Code for calculating the phases with the Linear model	23
A.3	Code for calculating the phases with the Revisited model	23
A.4	Code for calculating the phases with the model with longitudinal energy	25

Preface

This thesis is written as part of my bachelor assignment in the seminar Analyse, Stochastiek en Besliskunde and the course Bachelor Onderzoek Natuurkunde. The contents are accesible to all who have some knowledge in numerical mathematics and third year bachelor physics.

I will start this thesis by introducing the problem and the experiment which led to the problem, this will be done in section 1 and 2. In section 3 I will show the models used for simulating the experiment. Section 4 will be about the numerical method I used. I will show and discuss the results from the calculations in section 5, 6 and 7.

I want to thank Barry Koren, for his enthusiasm on this subject which was also new to him. In addition I want to thank him for his excellent guidance in the traject of the bachelor project and introducing me at the CWI. I also want to thank Tjerk Oosterkamp for introducing me to this subject and for never being out of enthusiasm and useful ideas. At last I want to thank Bas Edixhoven for introducing me to Pari/GP and for his different view on the mathematical part of the problem.

1 Introduction

The goal of my investigation is to calculate the phase difference an electron gets when traveling from the tip of a nanotube emitter to a screen and to compare this with the experimental results. This problem came from an investigation by E.Heeres et al.¹ They looked at electron emission from carbon nanotubes placed in an electric field. In the emission pattern they found possible interference lines. Numerical simulations by E. Heeres et al. were done to see whether these fringes are due to Young's interference, but no satisfactory results came from this. I am going to simulate the experiment with a powerful numerical integration rule and based on the results I will look whether the model needs to be improved.

2 Closed Multiwalled Carbon Nanotubes

E. Heeres et al. studied the effects of a closed cap on field emission from carbon nanotubes. A nanotube placed in an electric field, of sufficient strength, emits electrons from the tip. In the experiment the emission was imaged on a phosphor screen. It was posed that for certain groups of carbon nanotubes there exist separate electron beams leading to spots on the screen. These beams would originate from ultra small emission sites at the pentagons in the cap. These emission sites are shown in a simplified model in Figure 1.

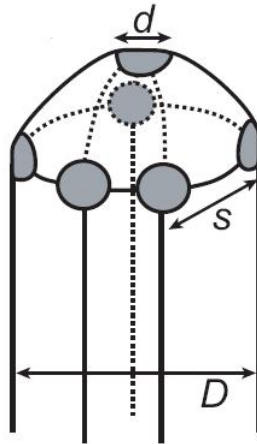


Figure 1. Simplified model of the tip of a nanotube, with in grey the electron emission spots

The electric field was generated using an extraction voltage V_{ext} . And imaging with field emission microscopy led to the following figure.

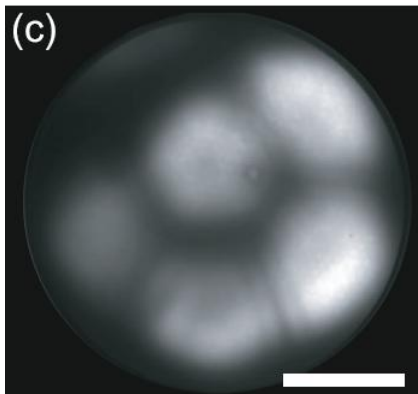


Figure 2. Field emission microscope pattern of the electron emission of the nanotube. The size of the scalebar represents 5 nm.

In Figure 2 we see spots due to the emission areas, and we also see lines between adjacent spots. It was discussed that these lines should be attributed to Young's interference between electrons. We can look at this theoretically and simulate the interference pattern fringes. Thus we can compare the experimental results to the results with Young's interference.

Work done by E. Heeres et al, led to a 2-D model of the experiment but not to satisfactory conclusions. They also showed that at one micrometer from the screen, the electron possesses 99.6% of its final energy. We will use this result to estimate the phase an electron gets.

3 Models

3.1 2-D model

For simulating the interference pattern fringes I used the model constructed by E. Heeres et al. In that model the emitter and the extractor are modeled as concentric spheres with different radii. Notice that the experimental shapes of the emitter and the extractor are not exactly spherical, thus the simulated parameters need not to be equal to the experimental parameters. With this model we can analytically calculate the trajectories and phases from electrons emitted from 2 point sources. What I want to calculate is the phase difference between these electrons when they reach the extractor in the same point.

I use the model in 2 dimensions, thus the spheres will be concentric circles. And we have coordinates:

$$x = r \cos \theta, \quad (1)$$

$$y = r \sin \theta. \quad (2)$$

The model defines two electron emission sites at angles $\theta = \theta_1$ and $\theta = \theta_2$, both with $r = R_{\text{tip}}$. We also define a screen position $(R_{\text{screen}}, \theta_3)$. The results of the model are given in relative angles $\Delta\theta_i = \theta_3 - \theta_i$ ($i = 1, 2$). When an electron leaves from the emitter, it has an energy which consists of a part parallel to the surface and a component perpendicular to the surface of the emitter, $E_{\text{tot}} = E_{\parallel} + E_{\perp}$. In the model the component perpendicular to the

surface is neglected, so $E_{\text{tot}} = E_{\parallel}$. When we find E_{\parallel} we can compute the track of the electron.

In this model the electric field generated by a voltage on the extractor is

$$\mathbf{E}(\mathbf{r}) = \frac{c_1}{r^2} \hat{\mathbf{r}}, \quad (3)$$

where $c_1 = \frac{R_{\text{screen}} R_{\text{tip}}}{R_{\text{screen}} - R_{\text{tip}}} V_{\text{ext}}$ with V_{ext} the voltage which is used to extract the electrons and $\hat{\mathbf{r}}$ the unit vector in the direction of \mathbf{r} . This electric field implies that the electron is in a central force field. In the derivation the solution of a mass moving in a central force field is used. The solutions are Kepler Orbits and the following track was found:

$$r = \frac{p}{-1 + \epsilon \cos \theta}, \quad (4)$$

where p and ϵ are defined as:

$$p_i = \frac{(r_0 m_e v_{0,i})^2}{m_e e c_1}, \quad (5)$$

$$\epsilon_i = 1 + \frac{r_0 m_e v_{0,i}^2}{e c_1}, \quad (6)$$

with $r_0 = R_{\text{tip}}$ and $v_{0,i} = \sqrt{\frac{2E_{\parallel,i}}{m_e}}$, the initial speed, e the charge of an electron and m_e the electron mass. The transversal energy $E_{\parallel,i}$ is given by the following expression:

$$E_{\parallel,i} = \frac{e c_1 R_{\text{screen}} (1 - \cos \Delta \theta_i)}{2 R_{\text{tip}} R_{\text{screen}} \cos \Delta \theta_i - 2 R_{\text{tip}}^2}. \quad (7)$$

This determines the track of the electron completely. The phase of the electron also depends on its velocity, which follows from the model as:

$$v(r)_i = \sqrt{\frac{2E_{\text{kin},i}(r)}{m_e}} = \sqrt{\frac{2}{m_e}} \sqrt{E_{\parallel,i} + e V_{\text{ext}} - e c_1 \left(\frac{1}{r} - \frac{1}{R_{\text{screen}}} \right)}. \quad (8)$$

To calculate the phase an electron gets when it reaches the screen, we integrate the wavevector:

$$\varphi_i = \frac{m_e}{\hbar} \int_{R_{\text{tip}}}^{R_{\text{screen}}} v(\mathbf{x}(r))_i |\mathbf{x}'_i(r)| dr, \quad (9)$$

where $\mathbf{x}(r)$ is the parametrisation of the electron track and \hbar the constant of Planck. From the equation of the track the model concludes that:

$$|\mathbf{x}'_i(r)| = \sqrt{\frac{-r^2 + \epsilon_i^2 r^2 - 2p_i r}{\epsilon_i^2 r^2 - p_i^2 - 2p_i r - r^2}}. \quad (10)$$

With this we can numerically integrate and thus find the phase that one electron gets when traveling to the screen.

3.2 Linear model

For testing the numerical method I made a model in which the electron track is not a hyperbolic Kepler orbit but a linear orbit. I made the same assumptions as in the 2-D model, so we consider the set up as 2 concentric spheres. The same electric field also applies to this situation. I neglect the initial energy: $E_{\parallel} = E_{\perp} = 0$. Because I am modelling a linear track I assume that the electron has the same velocity as in the 2-D model, but now in the direction of the endpoint. Then I get the same expression for the phase of an electron.

$$\varphi = \frac{m_e}{\hbar} \int v(r) dS. \quad (11)$$

We parametrize this integral over a line from the emitting point to the point where the electron reaches the screen, which all have been chosen as in the previous section. Thus we have for an electron leaving at angle θ_1 the following start and end points,

$$x(0) = R_{\text{tip}} \cos \theta_1, \quad (12)$$

$$x(1) = R_{\text{screen}} \cos \theta_3, \quad (13)$$

$$y(0) = R_{\text{tip}} \sin \theta_1, \quad (14)$$

$$y(1) = R_{\text{screen}} \sin \theta_3. \quad (15)$$

A linear parametrization for this set up is

$$x(t) = (1-t)R_{\text{tip}} \cos \theta_1 + tR_{\text{screen}} \cos \theta_3, \quad (16)$$

$$y(t) = (1-t)R_{\text{tip}} \sin \theta_1 + tR_{\text{screen}} \sin \theta_3, \quad (17)$$

$$t \in [0, 1], \quad (18)$$

which gives us

$$\varphi = \frac{m_e}{\hbar} \int_0^1 v(\mathbf{x}(t)) |\mathbf{x}'(t)| dt, \quad (19)$$

with

$$|\mathbf{x}'(t)| = \sqrt{(\sin \theta_3 R_{\text{screen}} - \sin \theta_1 R_{\text{tip}})^2 - (\cos \theta_3 R_{\text{screen}} - \cos \theta_1 R_{\text{tip}})^2}, \quad (20)$$

$$v(\mathbf{x}(t)) = \sqrt{\frac{2e}{m_e}} \sqrt{V_{\text{ext}} - c_1 \left(\frac{1}{r(t)} - \frac{1}{R_{\text{screen}}} \right)}, \quad (21)$$

$$r(t) = \sqrt{(t \sin \theta_3 R_{\text{screen}} + (1-t) \sin \theta_1 R_{\text{tip}})^2 + (t \cos \theta_3 R_{\text{screen}} + (1-t) \cos \theta_1 R_{\text{tip}})^2}. \quad (22)$$

This gives us an equation for the phase difference which an electron receives under these particular assumptions. The main profit of this equation is that the $\mathbf{x}'(t)$ term is not dependent on t .

3.3 Revisited model

This model was constructed due to the results I got from the previously discussed models. Here I make the same assumptions as for the 2-D model. From these assumptions it was concluded in the 2-D model that the electron travels on a Kepler orbit. In this model I take the following equation for a Kepler orbit, which follows directly from classical mechanics:

$$r = \frac{B}{AB \cos(\theta - \theta_0) - 1}, \quad (23)$$

where $B = \frac{m_e l^2}{ec_1} = \frac{m_e (R_{\text{tip}} v_0)^2}{ec_1}$, A is a constant which is chosen according to the problem and $\theta_0 = \theta_i$ is the initial angle of the electron. We know that $r = R_{\text{tip}}$ when $\theta = \theta_i$, this implies that

$$A = \frac{m_e v_0^2 R_{\text{tip}} + ec_1}{R_{\text{tip}}^2 m_e v_0^2}. \quad (24)$$

From $v_0 = \sqrt{\frac{2E_{\parallel}}{m_e}}$ and because we choose the electron to be at R_{screen} when $\theta = \theta_3$ we find that:

$$E_{\parallel,i} = -\frac{1}{2} \frac{eR_{\text{screen}}^2 V_{\text{ext}} (\cos \Delta\theta_i - 1)}{\cos \Delta\theta_i R_{\text{screen}}^2 - R_{\text{screen}} \cos \Delta\theta_i R_{\text{tip}} - R_{\text{screen}} R_{\text{tip}} + R_{\text{tip}}^2}. \quad (25)$$

We want to calculate

$$\varphi_i = \frac{m_e}{\hbar} \int_{R_{\text{tip}}}^{R_{\text{screen}}} v(r)_i dS, \quad (26)$$

with

$$v(r)_i = \sqrt{\frac{2E_{\text{kin},i}(r)}{m_e}} = \sqrt{\frac{2}{m_e}} \sqrt{E_{\parallel,i} + eV_{\text{ext}} - ec_1 \left(\frac{1}{r} - \frac{1}{R_{\text{screen}}} \right)}. \quad (27)$$

I parametrize the integral by making use of the equation for the Kepler orbit, this leads to the integral

$$\varphi_i = \frac{m_e}{\hbar} \int_{\theta_i}^{\theta_3} v(r(\theta)_i)_i |r'(\theta)_i| d\theta, \quad (28)$$

with

$$r(\theta)_i = \frac{B}{AB \cos(\theta - \theta_i) - 1}, \quad (29)$$

and

$$|r'(\theta)_i| = \left| \frac{AB^2 \sin(\theta - \theta_i)}{(AB \cos(\theta - \theta_i) - 1)^2} \right|, \quad (30)$$

to solve for φ .

3.4 Longitudinal Energy

In all the previous models the assumption $E_{\perp} = 0$ was made. In the following model we take $E_{\perp} \neq 0$, this implies that $E_{tot} = E_{\parallel} + E_{\perp}$. In this case we have to take account for tunneling of the electrons, which is shown in Figure 3.

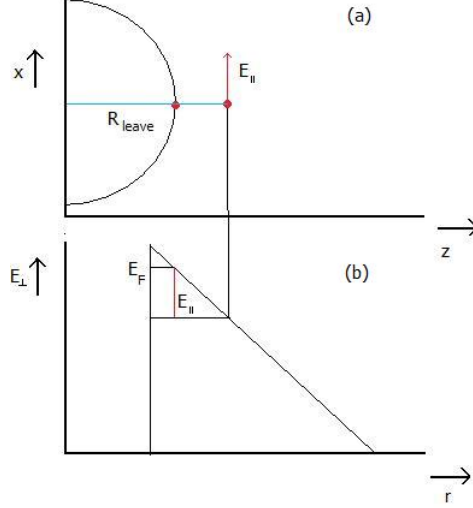


Fig. 3 Illustration of the tunneling of electrons out of the nanotube. The part on (a) shows the nanotube and the positions the electron leaves from. R_{leave} indicates the radius at which the electron leaves in polar coordinates. The transversal energy of the electron is also shown. In (b) the tunnel barrier is shown. Here r denotes the radius in polar coordinates. In this figure I assumed that $E_{tot} = E_F$, the Fermi-energy.

In this Figure I illustrated the tunneling of the electrons. This effect leads to a different radius at which the electron leaves, R_{leave} . By quantum mechanics, R_{leave} is given by

$$R_{leave} = R_{tip} + \frac{E_{\parallel} R_{tip}^2}{c_1}. \quad (31)$$

In Figure 3(a) the nanotube is illustrated with the different radii from which the electron can leave. In Figure 3(b) the tunneling barrier is shown which is responsible for the different radius at which the electron leaves.

In this model we fix the angle at which the electron leaves, θ_i . Then we know from (25) and (31)

$$\Delta\theta_i = \arccos \left(\frac{-2\frac{E_{\parallel,i}}{e} R_{screen} R_{leave} + 2\frac{E_{\parallel,i}}{e} R_{leave}^2 - R_{screen}^2 V_{ext}}{R_{screen} (-2R_{screen} \frac{E_{\parallel,i}}{e} - R_{screen} V_{ext} + 2\frac{E_{\parallel,i}}{e} R_{leave})} \right), \quad (32)$$

and the angle at which the electron reaches the screen, θ_3 , is given by

$$\theta_3 = \theta_i \pm \Delta\theta_i. \quad (33)$$

Now we can use (28),(29) and (30) to calculate φ_i with

$$A = \frac{m_e v_0^2 R_{leave} + e c_1}{R_{leave}^2 m_e v_0^2}, \quad (34)$$

$$B = \frac{m_e(R_{\text{leave}}v_0)^2}{ec_1}. \quad (35)$$

With this I calculate the phase of the electron for each $(E_{\parallel}, E_{\perp})$ with $E_{\text{tot}} = E_{\parallel} + E_{\perp}$. I also calculate the angle at which the electron reaches the screen and R_{leave} .

4 Numerical Method

The 2-D model leads us to an equation for the phase difference of the electrons. This is an integral which is recognized as an elliptic integral, which is computed numerically. For the numerical integration I used the double exponential method. This method makes use of the Trapezium Rule for numerical integration.

If we have the problem $y = \int_{t_0}^{t_m} f(t)dt$ the Trapezium Rule with stepsize h is given by:

$$w_1 = \frac{h}{2}(f(t_0) + f(t_1)), \quad (36)$$

where w_n is the approximation of $\int_{t_0}^{t_1} f(t)dt$. The rule is illustrated in the following figure:

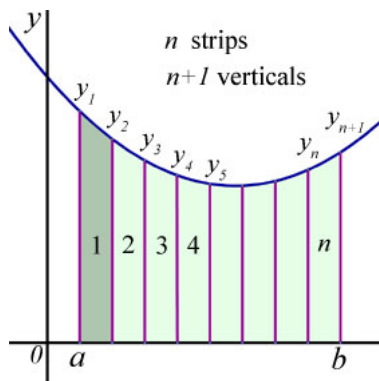


Fig. 4 Illustration of the Trapezium Rule. The Rule divides the interval in subintervals and approximates the area of each subinterval under the function as a trapezium.

By using the Trapezium Rule, we divide the interval in n subintervals. In each of these subintervals we approximate the area enclosed as a trapezium. The truncation of the Trapezium Rule is of order 2, but we can notice by the way the Trapezium Rule is constructed that there exist functions for which the Trapezium Rule works extremely well. The functions for which the rule works well are analytic functions over the real line that approach zero rapidly in the tails. This is what the Double exponential method makes use of.

Theorem 4.1 (Double exponential). *Let f be a function defined on the interval $[-1, 1]$, holomorphic on $D(0, 2) = \{z \in \mathbb{C}, |z| < 2\}$, then for every $n \geq 1$*

$$\left| \int_{-1}^1 f(x)dx - \sum_{k=-n}^n a_k f(x_k) \right| \leq (e^4 \sup_{D(0,2)} |f|) \exp\left(-\frac{5n}{\log(5n)}\right), \quad (37)$$

with $h = \frac{\log(5n)}{n}$, $a_k = \frac{h \cos(kh)}{\cosh(\sinh(kh))}$ and $x_k = \tanh(\sinh(kh))$.

Proof. Proof by P. Molin et al.⁴

This theorem shows that the error which is introduced by numerically integrating reduces exponentially in the stepsize used. With this method we can calculate integrals in thousands of digits accurately, as long as the integrand is regular. The domain over which we integrate may be non-compact, and the end points may have singularities. I used this method pre-programmed in the open source software Pari/GP to calculate the phase difference of the electrons.

5 Results

We want to simulate the interference pattern which occurs between the spots on the screen. To see whether we have interference we fix two emission spots on the emitter. Then, for 2000 points on the screen, we calculate the phase difference between electrons leaving from these spots when they reach the screen. Because we are interested whether the electrons interfere constructively or destructively we take the phase difference modulo 2π . I calculated all angles in radians. Doing this I found the following.

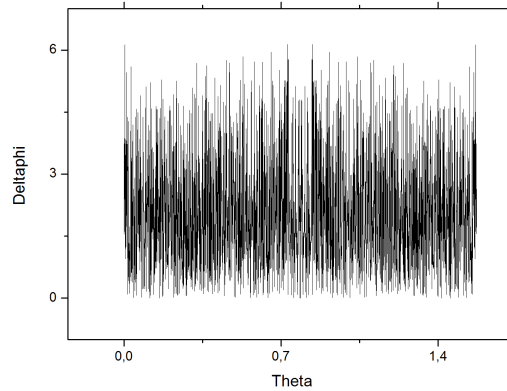


Fig. 5 Graph of the phase difference modulo 2π of two electrons being emitted at R_{tip} and angles 0.1 and $\frac{\pi}{2} - 0.1$ versus the angle where they reach the screen according to the 2-D model

Figure 5 shows the graph of the phase difference of two electrons which were emitted at $R_{\text{tip}} = 4.5\text{nm}$ and angles 0.1 and $\frac{\pi}{2} - 0.1$ versus the angle at which they reach the screen, $R_{\text{screen}} = 24\text{mm}$. In this calculation I took $V_{\text{ext}} = 500\text{V}$.

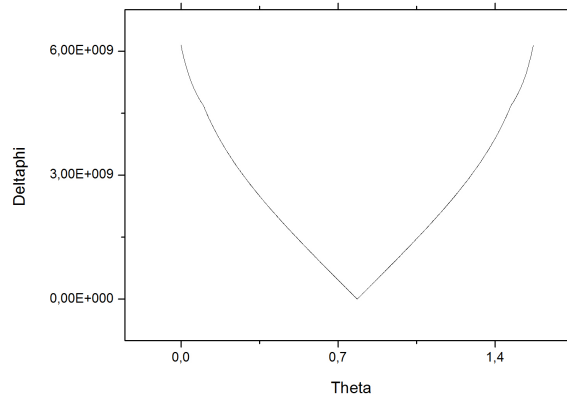


Fig. 6 Graph of the phase difference of two electrons being emitted at R_{tip} and angles 0.1 and $\frac{\pi}{2} - 0.1$ versus the angle where they reach the screen according to the 2-D model

I also looked at the phase difference without the modulo 2π taken into account. Then I get the graph in Figure 6. In Figure 7 I calculated the phase that one electron gets from leaving at angle 0.1 .

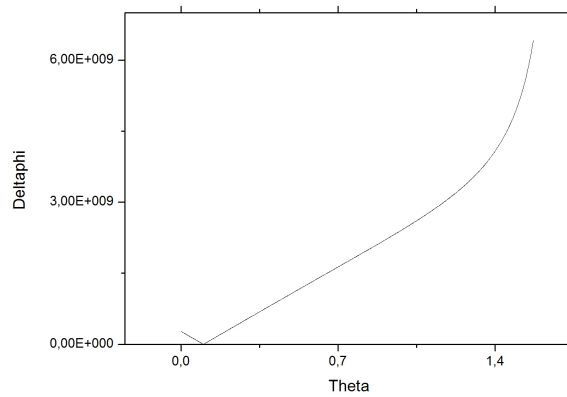


Fig. 7 Graph of the phase one electron gets when it is emitted at R_{tip} and angle 0.1 versus the angle where they reach the screen according to the 2-D model

I did the same calculation for a small range in the middle of the screen, where I also discretised this region in 2000 points. This is shown in Figure 8.

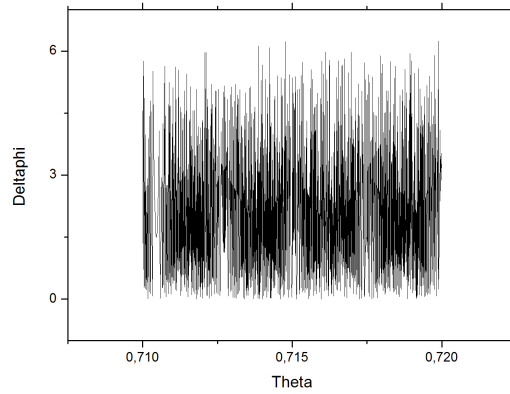


Fig. 8 Graph of the phase difference modulo 2π of two electrons being emitted at R_{tip} and angles 0.1 and $\frac{\pi}{2} - 0.1$ versus the angle where they reach the screen according to the 2-D model

Using the same model I simulated the screen at a distance of 1 micrometer instead of 24 millimeter. This is shown in Figure 9 .

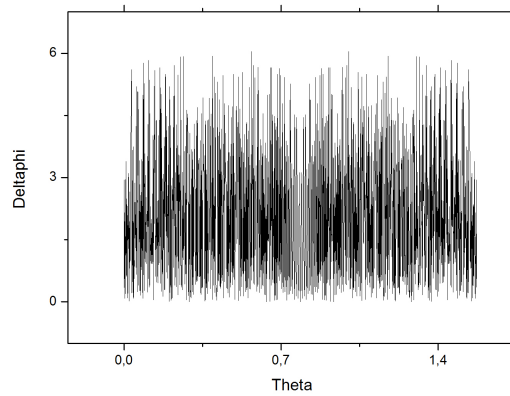


Fig. 9 Graph of the phase difference modulo 2π of two electrons being emitted at R_{tip} and angles 0.1 and $\frac{\pi}{2} - 0.1$ versus the angle where they reach the screen which is at a distance 1 micrometer according to the 2-D model

Simulations with the model for the linear track were made with the same set-up and $R_{screen} = 24\text{mm}$. The result is shown in Figure 10.

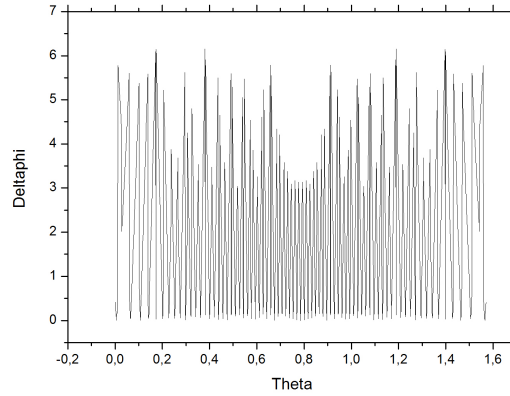


Fig. 10 Graph of the phase difference modulo 2π of two electrons being emitted at R_{tip} and angles 0.1 and $\frac{\pi}{2} - 0.1$ versus the angle where they reach the screen. Here the model for the linear track was used.

These simulations were also done with the screen at a distance of 2 cm and 2 m. The difference between these two graphs is shown in Fig. 11.

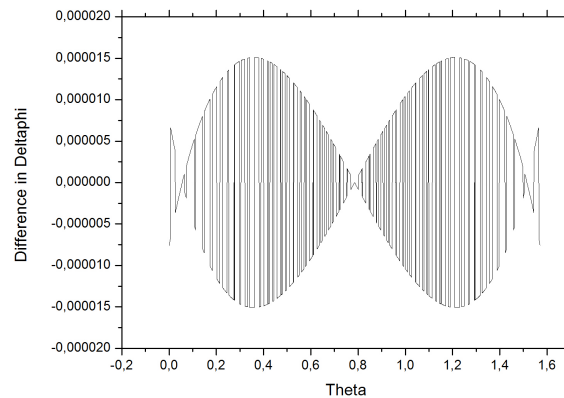


Fig. 11 Graph of the difference of $\Delta\varphi$ between the simulation with the screen at 2 cm and the simulation with the screen at 2 m versus the angle where the electrons reached the screen. According to the linear model

In Figure 12 it is shown which phase an electron gets when reaching the screen, according to the linear model.

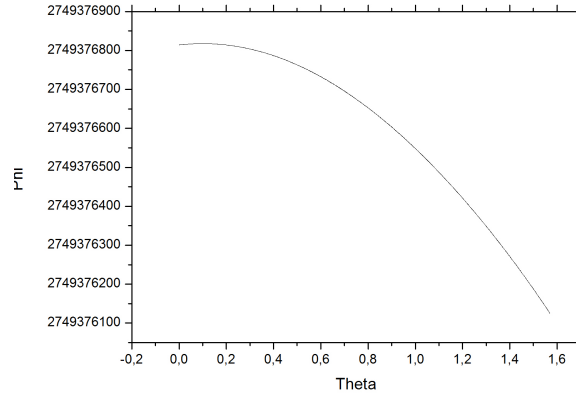


Fig. 12 Graph of the phase one electron gets, according to the linear model, when it is emitted at R_{tip} and angle 0.1 versus the angle where they reach the screen

For the Revisited model I also simulated the experiment with the same set up. Doing this I found Figure 13.

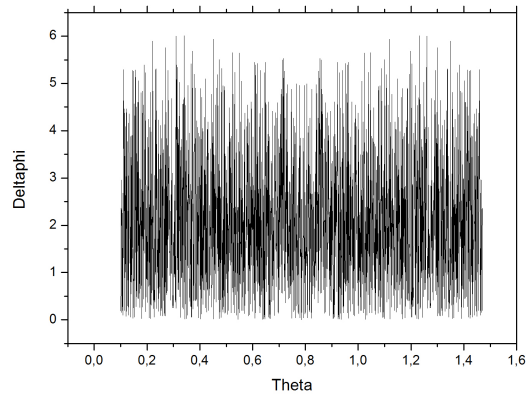


Fig. 13 Graph of the phase difference modulo 2π of two electrons being emitted at R_{tip} and angles 0.1 and $\frac{\pi}{2} - 0.1$ versus the angle where they reach the screen according to the Revisited model.

In Figure 14 the phase an electron gets when traveling to the screen, according to the Revisited model, is shown.

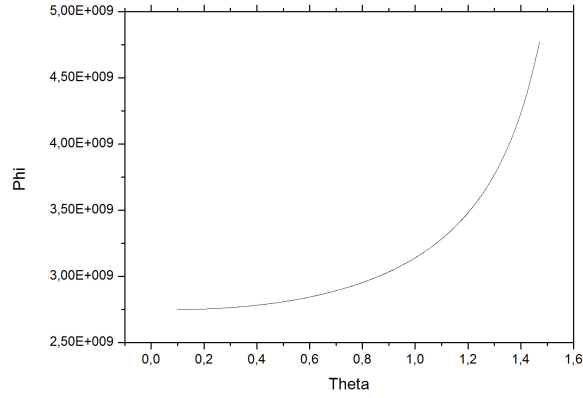


Fig. 14 Graph of the phase one electron gets when it is emitted at R_{tip} and angle 0.1 versus the angle where they reach the screen according to the Revisited model

I did the same for the model with the longitudinal energy included. I used $E_{tot} = E_F$ and $\theta_1 = 0.44$ which is the edge of an emission site. The result is shown in Figure 15.

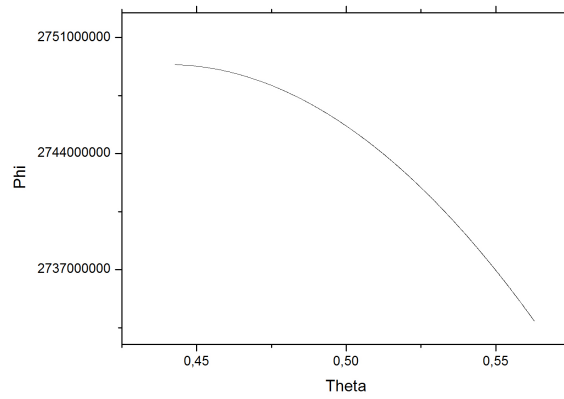


Fig. 15 Graph of the phase one electron gets when it is emitted at R_{tip} and angle 0.44 versus the angle where they reach the screen according to the model with longitudinal energy. In this simulation $E_{tot} = E_F$.

In Figure 16 the plot of R_{leave} versus $E_{||}$ is shown.

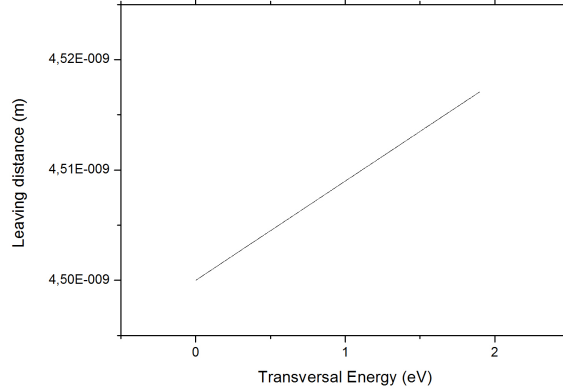


Fig. 16 Graph of R_{leave} versus E_{\parallel} calculated from the model with longitudinal energy. In this simulation $\theta_1 = 0.44$ and $E_{\text{tot}} = E_F$.

6 Discussion

The goal of the simulations is to investigate whether the observed fringes are because of Young's interference. The principle of Young's interference is shown in Figure 17.

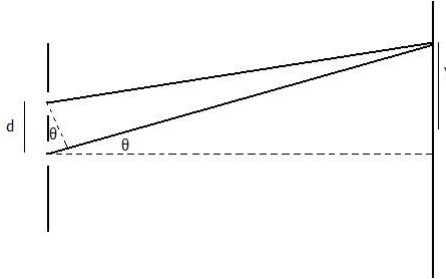


Fig. 17 Illustration of Young's interference. With d the distance between the openings and y the distance at which the beam hits the screen.

In this illustration d is the distance between the cracks and y is the distance at which the beam hits the screen. The phase difference between the two beams can be calculated by

$$\Delta\varphi = d \sin \theta. \quad (38)$$

This leads to an interference pattern with maxima if $d \sin \theta = n\lambda$ with $n \in \mathbb{N}$ and λ the wavelength. The maxima and minima are a result of the path difference between the beams. The expectation is that the fringes in Figure 2 are also caused by this principle of path difference. This is what I wanted to investigate by simulating the paths of the electrons.

When we look at Figure 2 we see at most 10 fringes. Though in Figure 5 and Figure 6, we see thousands of fringes, each time the line passes π . The simulation gives us a lot more interference fringes than we expect. This can be

due to the model, or a numerical error. It would also be possible that the interference we see in the experiment is not because of Young's interference.

We can expect what phase an electron gets when traveling from the tip to the screen. We know that at 1 micrometer from the emitter, the energy of the electron is 99.6% of the energy it has at the screen. We can estimate the energy at the screen as $E_{\text{final}} = 500\text{eV} = 8 \cdot 10^{-17}\text{J}$. The closer the electron gets to the screen, the greater the contribution to the phase becomes. So we estimate the phase as if the electron travels with energy E_{final} at the whole track. Then we get

$$E_{\text{final}} = \frac{\hbar^2(2\pi)^2}{2m\lambda^2}, \quad (39)$$

so

$$\lambda \approx \frac{h}{\sqrt{2mE_{\text{final}}}} \approx 5 \cdot 10^{-11}. \quad (40)$$

This means we assume a constant wavelength, and so the phase becomes

$$\varphi = \frac{R_{\text{screen}}}{\lambda} \approx \frac{R_{\text{screen}}}{5 \cdot 10^{-11}} \approx 5 \cdot 10^8. \quad (41)$$

This approximation is when the electron travels on the shortest path possible. The path is linear, thus the actual phase can be an order higher as the approximation. When we compare this with the results in Figure 7 we see that a big part of the graph is below our estimation. Also at angle 0.1 the calculated phase of the electron is identical to zero. This is impossible in the experimental set up because that would imply that the electron would not have traveled at all.

The graph in Figure 10 shows us that also in the Linear Model we have a lot of oscillations. We can explain these oscillations with Figure 11. There we see the phase of the electron decrease an order 100. This decrease results in the oscillations modulo 2π . This can also be used to explain the oscillations in Figure 5. The large increase by an order 10^9 in Figure 7 is responsible for most of the oscillations in Figure 5. We can see that this increase comes from the parametrisation used in the 2-D model, equation (10). If $\Delta\theta_i = 0$ we have $p_i = 0$ and $\epsilon_i = 1$, thus

$$|\mathbf{x}'_i(r)| = \sqrt{\frac{-r^2 + r^2}{r^2 - r^2}}, \quad (42)$$

which is modeled as identically zero. Also the parametrisation is an increasing function of $\Delta\theta_i$. This is responsible for most of the increase in Figure 7.

We take a closer look at the parametrisation by investigating the equation of the hyperbola, (4). This is derived as a Kepler orbit. In the derivation of the Kepler orbits the origin of the coordinate system is taken to be the focus of the ellipse or hyperbola. But the origin of the coordinate system in which we integrate is not the focus of the hyperbola. This leads to an incorrect parametrisation of the track of the electron. This might be the reason why we have this increasing line from zero in Figure 7.

The Revisited model was constructed due to these observations. In this model the correct origin of the coordinate system is used. Though Figure 13 shows that this model does not give us a lot of improvement regarding the phase difference modulo 2π . We still see a lot more oscillations as expected from the

experiment. We can see where this comes from by looking at Figure 14. The phase an electron gets from traveling to the screen increases an amount of $2 \cdot 10^9$. This leads to the oscillations in Figure 14. The Revisited model does solve the physical problem that occurred with the 2-D model, the phase of one electron converges to approximately $2 \cdot 10^9$ when $\Delta\theta$ goes to 0, as shown in Figure 14. This improvement also implies that a singularity at $\Delta\theta = 0$ exists, because in this case we do not have a hyperbola and the derivation of the Kepler orbits can not be used. We see this in the model, the integrand goes to infinity when $\Delta\theta$ goes to 0.

The graphs in Figure 6,7 and 12 are smooth, so the oscillations in Figure 5 are not because of oscillations in the numerical solution. We can also check the numerical method on physical properties. Physically, the interference pattern should not change in the far field. This is illustrated in Figure 18.

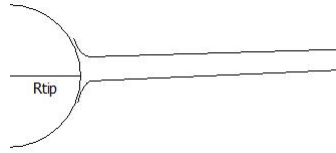


Fig. 18 Illustration of Far Field properties. When $R_{\text{screen}} \gg R_{\text{tip}}$ the paths of the electrons are almost parallel.

As shown in Figure 18, when $R_{\text{screen}} \gg R_{\text{tip}}$ the paths of the electrons are almost parallel. This implies that the pattern does not change in the far field. To check the method I looked at the far field using the Linear Model, and as shown in Figure 11 the method conserves this property for $R_{\text{screen}} = 2\text{cm}$ and $R_{\text{screen}} = 2\text{m}$. In Figure 9 we can also see this property, if I simulate the screen at 1 micrometer from the tip we still see heavy oscillations. Thus the pattern will show heavy oscillations for all $R_{\text{screen}} > 1\mu\text{m}$ and the part of the path where the energy is almost constant contributes the least to the pattern.

One could also consider that the pattern is not due to interference between the electrons, but because of diffraction from the electrons. If the phenomenon would be diffraction, the electron leaving at the emitter would have diffraction. This would imply that this is true for every electron leaving the emitter, so we should expect that the fringes are also very close to the center of the emitting areas. This is not the case as we have observed, the fringes are mostly between the spots, and with diffraction one would expect to see the same pattern to continue at the spots. Thus I would not expect that the fringes are due to diffraction.

Another possibility to improve the model is considering the longitudinal energy of the electron. In the 2-D model we neglect the longitudinal energy. If we do not neglect the longitudinal vector, we get 2-D vectors that determine the track. This property could reduce the oscillations. I simulated this with the model with longitudinal energy. Though from Figure 15 we see a decrease of $2 \cdot 10^7$ which will cause a lot of oscillations modulo 2π . I simulated Figure 15 with $\theta_1 = 0.44$ which is at the edge of the emission area and $E_{\text{tot}} = E_F$. In Figure 15 though the electron only reaches $\theta_3 \approx 0.58 < \frac{\pi}{4}$. This implies that the electrons from two emission sites do not interfere with each other when

$E_{\text{tot}} \leq E_F$, according to the simulations. From quantum mechanics an electron with energy $E_{\text{tot}} = E_{\parallel} + E_{\perp}$ has a chance to leave the nanotube given by,

$$P_{\text{leave}}(E_{\text{tot}}, E_{\parallel}) = \frac{1}{\exp\left[\frac{E_{\text{tot}} - \mu}{k_B T}\right] + 1} \cdot e^{-\frac{E_{\parallel}}{D}}, \quad (43)$$

where μ is the chemical potential and $D = 0.34$ eV is determined experimentally for $V_{\text{ext}} = 470V$. This implies that for larger E_{tot} the chance to leave rapidly decreases.

With this model the electrons from different sites do not interfere. This can also be seen in Figure 1, only at the bottom the electrons overlap. Between all other sites the electrons do not overlap visibly and from that I expect that fringes are not because of Young's interference between two sites. I also expect that the fringes are because of interference of electrons from the same emission site. Interference of electrons from the same site is possible with $E_{\text{tot}} \leq E_F$ and will have the same properties as interference from 2 sites. The difference is that the minimum in the middle of two sites does not exist. This can be shown by experiments with the nanotube where V_{ext} will be increased. When the fringe pattern becomes smaller with exception of the middle minimum this would be a lead to interference of electrons from the same site.

Further investigation can be done on the model with longitudinal energy. One could investigate whether interference from the same emission site can be modeled. Doing this one should not only consider the phase an electron gets, but also the intensity at the screen. When using and summing this over all electrons leaving from the site one can determine whether the electrons from one site can interfere. If this does not lead to satisfactory results one could consider that the interference is due to impurities on the nanotube. This would also explain why in Figure 1 we do not see visible interference between all emission sites.

7 Conclusion

The double exponential numerical integration method has an exponentially decreasing error for regular functions which have a finite amount of singularities. The results we get from the calculations are qualitatively not affected by the numerical method. This double exponential method used in the open source software Pari/GP is a powerful tool for numerical integration in physical problems.

When simulating the experiment with the 2-D model we see a factor thousand more fringes as in the actual experiment. This is for a part due to the parametrisation of the model. In deriving the orbits of the electron traveling from the emitter to the screen, a coordinate system with the origin in the focus of the orbit was used. Though the coordinate system we use when integrating has its origin in the center of the emitter.

The Revisited model has its origin shifted and gives us physically correct properties around $\Delta\theta = 0$. Though this does not result in observing the expected amount of fringes. Most of the simulated fringes are not due to the

shifted origin but due to the massive increase in the phase an electron gets, when traveling to the screen, as the path length increases.

The model with longitudinal energy has the best physical properties. This model also decreases the amount of fringes, but the amount is still a lot higher than expected. One can also conclude from this model that the electrons from two emission sites can not interfere with each other due to Young's interference.

Further investigation can be done in this direction. The interference of electrons is the most probable explanation of the fringes as seen in the experiment. Looking if it is possible that electrons from the same emission site can interfere and modeling the interference of this occurrence is very useful in understanding this problem. Another interesting path is to look if the interference of the electrons is because of impurities in the nanotube. At least a next approach should be more experimental to understand the problem.

8 References

- [1] E. Heeres et al., unpublished manuscript.
- [2] C. Vuik et al., Numerieke Methoden voor Differentiaalvergelijkingen, VSSD, 2006.
- [3] G. Fowles & G. Cassiday, Analytical Mechanics, Brooks/Cole, 2005.
- [4] P. Molin, L'intégration numérique par la méthode double-exponentielle, 2010.
- [5] R. A. Adams, Calculus A Complete Course, Pearson Education, 2006.
- [6] D. J. Griffiths, Introduction to Quantum Mechanics, Pearson Education, 2004.
- [7] The PARI group, Pari/GP 2.5.0, <http://pari.math.u-bordeaux.fr/>, 2011.

A Pari/GP Codes

A.1 Code for calculating the phases with the 2-D model

```
\p 100
theta_start = 0
theta_end = Pi/2
theta_diff = theta_end - theta_start
n = 2000
chi = 0
e = 1.60217653*10^-19
m_e = 9.1093826*10^-31
h = 6.6260693*10^-34
hbar = h/(2*Pi)
R_screen = 1*10^-6
R_tip = 4.5*10^-9
V_ext = 500
c1 = (R_screen*R_tip*V_ext)/(R_screen-R_tip)
theta_1 = 0.09
theta_2 = Pi/2 - 0.1
E_F = 1.9
for (i = 0,n,theta_0 = theta_start + i*theta_diff/n;
Delta_theta_1 = abs(theta_0 - theta_1);
Delta_theta_2 = abs(theta_0 - theta_2);
E_tr_1 = abs(e*(c1*R_screen*(1-cos(Delta_theta_1)))
/(2*R_tip*R_screen*cos(Delta_theta_1)-2*R_tip*R_tip));
E_tr_2 = abs(e*(c1*R_screen*(1-cos(Delta_theta_2)))
/(2*R_tip*R_screen*cos(Delta_theta_2)-2*R_tip^2));
v_01 = sqrt((2*e*E_tr_1)/m_e);
v_02 = sqrt((2*e*E_tr_2)/m_e);
b_1 = 1 + (R_tip*m_e*v_01^2)/(e*c1);
b_2 = 1 + (R_tip*m_e*v_02^2)/(e*c1);
p_1 = (R_tip*m_e*v_01)^2/(m_e*e*c1);
p_2 = (R_tip*m_e*v_02)^2/(m_e*e*c1);
W_total_1 = e*E_tr_1+e*V_ext;
result_1 = intnum(r = R_tip,R_screen,sqrt(W_total_1-e*c1*(1/r-1/R_screen))*
sqrt((-r^2+b_1^2*r^2-2*p_1*r)/(b_1^2*r^2-p_1^2-2*p_1*r)));
W_total_2 = e*E_tr_2+e*V_ext;
result_2 = intnum(r = R_tip,R_screen,sqrt(W_total_2-e*c1*(1/r-1/R_screen))*
sqrt((-r^2+b_2^2*r^2-2*p_2*r)/(b_2^2*r^2-p_2^2-2*p_2*r)));
phi_1 = m_e/hbar*sqrt(2/m_e)*result_1;phi_2 = m_e/hbar*sqrt(2/m_e)*result_2;
mod_1 = phi_1/(2*Pi);
round_1 = truncate(mod_1);
mod_2 = phi_2/(2*Pi);
round_2 = truncate(mod_2);
final_1 = (mod_1-round_1)*2*Pi;
final_2 = (mod_2-round_2)*2*Pi;
delta_phi = abs(final_1-final_2);
writetex("resultaat",delta_phi);)
```

A.2 Code for calculating the phases with the Linear model

```

\p 20
theta_start = 0
theta_end = Pi/2
theta_diff = theta_end - theta_start
n = 2000
chi = 0
e = 1.60217653*10^-19
m_e = 9.1093826*10^-31
h = 6.6260693*10^-34
hbar = h/(2*Pi)
R_screen = 2
R_tip = 4.5*10^-9
V_ext = 500
c1 = (R_screen*R_tip*V_ext)/(R_screen-R_tip)
theta_1 = 0.1
theta_2 = Pi/2-0.1
for (i = 0,n,theta_0 = theta_start + i*theta_diff/n;
Delta_theta_1 = abs(theta_0 - theta_1);
Delta_theta_2 = abs(theta_0 - theta_2);
result_1=intnum(t = 0,1,sqrt(2/m_e)*sqrt(e*V_ext-e*c1*(1/sqrt
((t*sin(theta_0)*R_screen+(1-t)*sin(theta_1)*R_tip)^2+(t*cos(theta_0)
*R_screen+(1-t)*cos(theta_1)*R_tip)^2)-1/R_screen))*sqrt((sin
(theta_0)*R_screen-sin(theta_1)*R_tip)^2+(cos(theta_0)*R_screen-cos
(theta_1)*R_tip)^2));
result_2 = intnum(t = 0,1,sqrt(2/m_e)*sqrt(e*V_ext-e*c1*(1/sqrt
((t*sin(theta_0)*R_screen+(1-t)*sin(theta_2)*R_tip)^2+(t*cos(theta_0)
*R_screen+(1-t)*cos(theta_2)*R_tip)^2)-1/R_screen))*sqrt((sin
(theta_0)*R_screen-sin(theta_2)*R_tip)^2+(cos(theta_0)*R_screen-cos
(theta_2)*R_tip)^2));
phi_1 = m_e/hbar*result_1;
phi_2 = m_e/hbar*result_2;
mod_1 = phi_1/(2*Pi);
round_1 = truncate(mod_1);
mod_2 = phi_2/(2*Pi);
round_2 = truncate(mod_2);
final_1 =(mod_1-round_1)*2*Pi;
final_2 =(mod_2-round_2)*2*Pi;
delta_phi = abs(final_1-final_2);
writetex("deltaphiLineair",delta_phi);

```

A.3 Code for calculating the phases with the Revisited model

```

\p 100
theta_start = 0.1001
theta_end = Pi/2 - 0.1001

```

```

theta_diff = theta_end - theta_start
n = 2000
chi = 0
e = 1.60217653*10^-19
m_e = 9.1093826*10^-31
h = 6.6260693*10^-34
hbar = h/(2*Pi)
R_screen = 24*10^-3
R_tip = 4.5*10^-9
V_ext = 500
c1 = (R_screen*R_tip*V_ext)/(R_screen-R_tip)
theta_1 = 0.1
theta_2 = Pi/2 - 0.1
for (i = 0,n,theta_0 = theta_start + i*theta_diff/n;
Delta_theta_1 =theta_0 - theta_1;
Delta_theta_2 = theta_0 - theta_2;
E_tr_1 = (-1/2)*(R_screen^2*V_ext*(-1+cos(Delta_theta_1)))
/(cos(Delta_theta_1)*R_screen^2-R_screen*cos(Delta_theta_1)*
R_tip-R_screen*R_tip+R_tip^2);
E_tr_2 = (-1/2)*(R_screen^2*V_ext*(-1+cos(Delta_theta_2)))
/(cos(Delta_theta_2)*R_screen^2-R_screen*cos(Delta_theta_2)*
R_tip-R_screen*R_tip+R_tip^2);
v_01 = sqrt((2*e*E_tr_1)/m_e);
v_02 = sqrt((2*e*E_tr_2)/m_e);
b_1 = (m_e*(R_tip*v_01)^2+R_tip*e*c1)/(R_tip*e*c1);
b_2 = (m_e*(R_tip*v_02)^2+R_tip*e*c1)/(R_tip*e*c1);
p_1 = m_e*(R_tip*v_01)^2/(e*c1);
p_2 = m_e*(R_tip*v_02)^2/(e*c1);
W_total_1 = E_tr_1+V_ext;
result_1 = abs(intnum(T = theta_1,theta_0,sqrt(W_total_1-c1*
(1/(p_1/(b_1*cos(T - theta_1) - 1)) - 1/R_screen))*((p_1*b_1*
sin(T - theta_1))/((b_1*cos(T - theta_1)-1)^2))));
W_total_2 = E_tr_2+V_ext;
result_2 = abs(intnum(T = theta_2,theta_0,sqrt(W_total_2-c1*(
1/(p_2/(b_2*cos(T - theta_2) - 1)) - 1/R_screen))*((p_2*b_2*
sin(T - theta_2))/((b_2*(T - theta_2)-1)^2))));
phi_1 = abs(m_e/hbar*sqrt(2*e/m_e)*result_1);
phi_2 = abs(m_e/hbar*sqrt(2*e/m_e)*result_2);
mod_1 = phi_1/(2*Pi);
round_1 = truncate(mod_1);
mod_2 = phi_2/(2*Pi);
round_2 = truncate(mod_2);
final_1 = (mod_1-round_1)*2*Pi;
final_2 = (mod_2-round_2)*2*Pi;
delta_phi = abs(final_1-final_2);
writetex("resultaatextra",delta_phi);
writetex("resultaatphiextra",phi_1);
writetex("resultaatphiextra2",phi_2);)

```

A.4 Code for calculating the phases with the model with longitudinal energy

```

\p 100
E_par_start = 0
E_par_end = 1.9
E_diff = E_par_end - E_par_start
n = 2000
chi = 0
e = 1.60217653*10^-19
m_e = 9.1093826*10^-31
h = 6.6260693*10^-34
hbar = h/(2*Pi)
R_screen = 24*10^-3
R_tip = 4.5*10^-9
V_ext = 500
c1 = (R_screen*R_tip*V_ext)/(R_screen-R_tip)
theta_1 = 0.44
theta_2 = Pi/2 - 0.1
E_F = 1.9
d = 0.34
for (i = 1,n,E_par_0 = E_par_start + i*E_diff/n;
E_lod_0 = E_par_end - E_par_0;
R_leave = R_tip + E_par_0/(c1/R_tip^2);
Delta_theta_1 = acos((-2*E_par_0*R_leave*R_screen+2*E_par_0*
R_leave^2-R_screen^2*V_ext)/(R_screen*
(-2*R_screen*E_par_0-R_screen*V_ext+2*E_par_0*R_leave)));
theta_0 = theta_1 + Delta_theta_1;
v_01 = sqrt((2*e*E_par_0)/m_e);
b_1 = (m_e*(R_tip*v_01)^2+R_tip*e*c1)/(R_tip*e*c1);
p_1 = m_e*(R_tip*v_01)^2/(e*c1);
W_total_1 = E_par_0 + V_ext;
result_1 = abs(intnum(T = theta_1,theta_0,sqrt(W_total_1-c1*(1/
(p_1/(b_1*cos(T - theta_1) - 1)) - 1/R_screen))*((p_1*b_1*sin(T - theta_1))/
((b_1*cos(T - theta_1)-1)^2)))));
phi_1 = abs(m_e/hbar*sqrt(2*e/m_e)*result_1);
;writetex("thetafinal",theta_0);
writetex("phifinal",phi_1);)

```